

# Study of the relation between Mg content and dissolution kinetics of natural lime stone using $\mu$ XRF, $\mu$ XRD and $\mu$ XAS

H S Grunwaldt<sup>1</sup>, A Zimina<sup>2,3</sup>, J Göttlicher<sup>4</sup>, R Steininger<sup>4</sup> and J D Grunwaldt<sup>2,3</sup>

<sup>1</sup>Faculty of Agriculture, University of Applied Science Kiel, Germany

<sup>2</sup>Institute of Catalysis Research and Technology, Karlsruhe Institute of Technology, Germany

<sup>3</sup>Institute for Chemical Technology and Polymer Chemistry, Karlsruhe Institute of Technology, Germany

<sup>4</sup>ANKA Karlsruhe Institute of Technology, Germany

E-mail: anna.zimina@kit.edu

**Abstract.** The dissolution parameters of calcium carbonates play a key role in agriculture as they regulate the plant nutrients uptake and buffer the pH-value of the soil. The combination of  $\mu$ XRF,  $\mu$ XAS and  $\mu$ XRD mapping in the hard X-ray regime for the examination of both short- and long range order in natural limestones revealed that their dissolution properties depend both on the crystallinity of the mineral phases and their composition. The results particularly show that in many cases the presence of magnesium inhibits dissolution of the phases.

## 1. Introduction

Calcium carbonate as natural limestone plays an important role in agriculture [1,2]. Calcium carbonates regulate the pH-value of the soil, the availability of several plant nutrients like phosphates, and prevent the dissolution of hazardous elements like aluminum and heavy metals. On one hand, calcium deficiency causes damage to plants. Calcium excess in turn causes indirect damage, as it blocks the availability of micronutrients and can furthermore lead to magnesium and potassium deficiency.

Natural limestones consist primarily of calcite and aragonite ( $\text{CaCO}_3$ ), but may contain dolomite when the calcium ions are replaced by magnesium ions ( $\text{MgCa}[\text{CO}_3]_2$ ). It is well known that the crystal structure, crystallinity and Mg content influence the solubility of calcite carbonates [3-5], but there are inconsistencies in liming material evaluation [6,7]. Hence, in this study the particle size, chemical composition and crystallinity of different phases of limestones in their natural form are traced and linked to their effectiveness as fertilizer, judged by acid neutralization capacity measurements [6], a method nowadays applied in Europe (Commission Regulation (EU) 463/2013 : Method 14.2 EN 13971 and Method 14.3 EN 16357). A preliminary study on samples from Northern Germany, USA and the United Kingdom which show different reactivity and crystallinity, already visible by bulk X-ray diffraction and in the optical microscope, hint to the presence of structural selectivity due to size fractionating [3,4,6,8-10].

Detailed information on the distribution of magnesium and calcium in the sample can be obtained by applying X-ray fluorescence ( $\mu$ XRF) mapping on the 50  $\mu\text{m}$  length scale. Combining  $\mu$ XRF with X-ray diffraction ( $\mu$ XRD) and X-ray absorption ( $\mu$ XAS) measurements on the same length scale



provides a link between the chemical composition, the microcrystallinity and the calcium coordination of the sample. This helps to clarify the relation between the structure and the dissolution kinetics of natural limestones [11,12]. The crystal size influence on the dissolution behavior of the limestones can be followed by examining different sieve fractions of the same material.

## 2. Experimental and data analysis

The experiment was performed at the SUL-X beamline at ANKA, where it is possible to focus the beam to 50 $\mu$ m at 4.2keV using a cryogenically cooled Si(111) monochromator and Kirkpatrick –Baez mirror setup.  $\mu$ XRD was measured with an area detector, while  $\mu$ XRF and  $\mu$ XAS measurements were performed using a 7-element SiLi detector at the Ca K-edge at the same sample position. The experimental vessel was evacuated to  $2 \times 10^{-5}$  mbar to prevent the absorption of low energy photons in air, enabling recording of Mg  $K_{\alpha}$ -fluorescence at 1253.6eV. Samples were spread onto Kapton tapes and mapped with respect to Mg and Ca content at 4.2keV. Each point was analyzed by  $\mu$ XRD at 14 keV in transmission mode and  $\mu$ XAS at the Ca K edge at 4038.5eV in fluorescence mode, in order to relate the Mg content to the changes in crystalline structure and in electron density in the vicinity of the Ca atoms.

In this study 6 natural limestones were investigated. Milled calcite, dolomite, and aragonite were used as reference materials. The reactivity measurements were conducted as follows: 200 mg  $\text{CaCO}_3$ -equivalent treated with 10 ml citrate buffer at pH 4.1 (2 N citric acid, 2.5 sodium citrate) 30 min in Scheibler-Apparatus, released  $\text{CO}_2$  determined volumetrically and converted to % dissolved carbonate. For each sample  $\mu$ XRF mapping was performed inside 1x1 mm<sup>2</sup> optically preselected regions of interest with a 50x50 $\mu$ m<sup>2</sup> beam.  $\mu$ XRD mapping was performed on the same 1x1mm<sup>2</sup> area in transmission. A smaller area of 0.24x0.24mm<sup>2</sup> was chosen for the  $\mu$ XAS mapping based on  $\mu$ XRF and  $\mu$ XRD, the XANES spectrum up to  $k = 8 \text{\AA}^{-1}$  was recorded at each point of the mesh in 40 $\mu$ m steps.

The elemental distributions of Mg and Ca were calculated using the integrated intensity of the relevant  $K_{\alpha}$  fluorescence lines. The XRD pattern was calibrated with the help of  $\text{LaB}_6$  milled powder and radial and azimuthal integration performed using the IgorPro Nika software package [13].

The natural limestones can strongly deviate from perfect randomly oriented powders, and this induces changes in the relative intensity of the diffraction peaks due to the presence of large crystallites. The presence of specific mineral phases was confirmed if the significant intensity of (104), (2-13) and (202) for calcite/dolomite and (111) and (102) for aragonite diffraction peaks were observed during measurement. The XRD maps were calculated for different components using the intensities of the (104) diffraction lines of calcite and dolomite and (111) of aragonite. Additionally, the crystallinity of each sample was deduced by analyzing the radial intensity distribution of the (104)/(102) diffraction line.

The Ca K-edge XAS data were preliminarily processed using the Athena software [14] and calibrated to calcite and dolomite standards. The XAS spectra of different areas were preliminarily examined using principal component analysis (PCA built-in function in Athena) and observed components were compared to the reference materials. The XAS chemical component maps were calculated based on linear combination analysis (LCA) in the energy range from -20 eV to 100 eV relative to the absorption edge, using the spectra of calcite, dolomite and components from the previous PCA procedure. The unavoidable effect of self-absorption at these photon energies has to be considered. The assignment of the chemical state of the Ca ion is based on the energy position of the characteristic spectral features and not on their relative intensities. In such a way the difference in damping of the post-edge intensity at every single mapping point might be compensated by selection of sample areas with a similar thickness and by identical preparation of the reference materials.

## 3. Results and discussion

In this study 6 natural limestones of three different sieve fractions (350-100 $\mu$ m, 100-50 $\mu$ m and below 50 $\mu$ m) were investigated: Oker, Tilcon, Salzhemmendorf, Columbia River Carbonate Calder (CRC Calder), Columbia River Carbonate Wauconda (CRC Wauconda, 1mm and 100-50 $\mu$ m), Dolomite

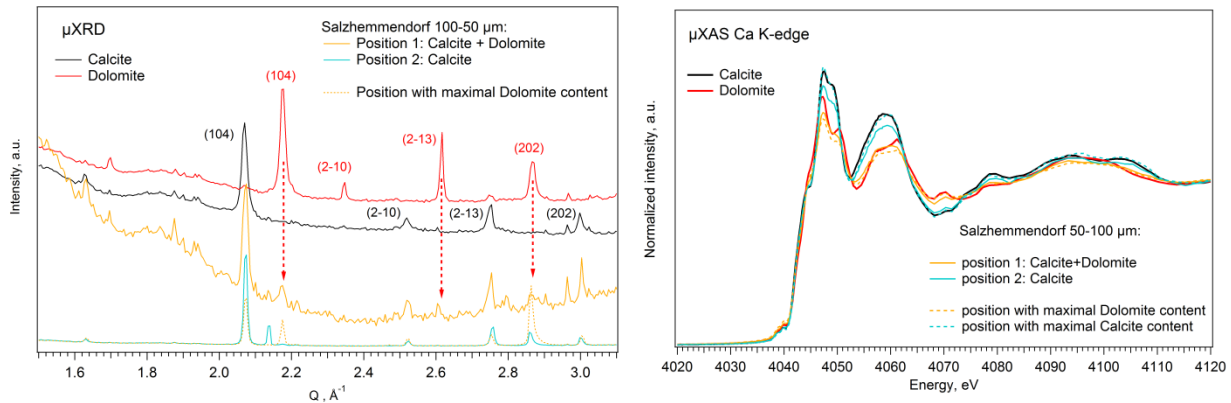


**Figure 1.** XRD pattern (left) and XAS Ca K spectra (right) of representative point of calcitic Salzhemmendorf, 100-50  $\mu\text{m}$  sieve fraction.

**Table 1.** Characteristics of the studied materials deduced from  $\mu\text{XRD}$  and  $\mu\text{XAS}$  and their reactivity as a fertilizer, the relative phase content is estimated based on statistics of the LCA of  $\mu\text{XAS}$  data, with a detection limit of  $\pm 5\%$  due to experimental uncertainty.

<i>Limestones</i>	<i>Main phase</i>	<i>Additional phase</i>	<i>Reactivity</i>
Calcite Oker	Calcite, polycrystalline	10% Dolomite, 40% Mg containing Calcite, 50-100 $\mu\text{m}$	high
Dolomite Tilcon	Dolomite with Mg deficit, monocrystalline, all sizes	>5% Calcite, 350-100 $\mu\text{m}$	low
Calcite Salzhemmendorf	Calcite, polycrystalline, all sizes	20% Dolomite, 350-100 $\mu\text{m}$	high
CCR Wauconda,	Calcite, monocrystalline, 350-100 $\mu\text{m}$	30% Mg containing Calcite, polycrystalline	low, increasing with decrease of sieve fraction
CCR Calder	Mg containing Calcite, all sizes	35% Calcite, polycrystalline, all sizes	low, increasing with decrease of sieve fraction
Dolomite Jettenberg,	Dolomite, polycrystalline	10% Calcite, polycrystalline	low

Jettenberg (100-50 $\mu\text{m}$ ). As an example the results on the Salzhemmendorf 100-50  $\mu\text{m}$  sieve fraction are shown here in detail.

Figure 1 shows the XRF Mg map normalized to the total Ca and Mg intensity, in order to trace the location of the dolomite phase in the Salzhemmendorf sample (100-50  $\mu\text{m}$ ). The XRD component maps of the same area are shown, the smaller area where the  $\mu\text{XAS}$  measurements were conducted is marked with white boxes. At the bottom of figure 1 the XRD patterns and XAS spectra of 2 selected points on the maps where the most pronounced difference in XRD signal was measured are shown. The XAS spectra at these 2 points reveal the presence of dolomite and calcite and they are linked to the Mg content plotted as an XRF map. Note furthermore the difference in the XAS component map compared to the XRD phase map. This might be due to the different penetration length of these two methods and insensitivity of the XRD measurements to thin amorphous surface layers. Hence, a combination of XRF, XRD and XAS seems to be beneficial.

All the samples were processed in the same way and detailed thorough analysis of the data was performed to obtain a representative picture of the investigated material and a detailed view of the structure at various sieve fractions. Based on this detailed analysis we concluded that high Mg concentration causes the formation of the dolomite related structure which is supported by XRD and XAS methods. The deficit of Mg (concentration below certain dissolution limit) leads to the formation

of calcite-like crystalline structures (“modified calcite”,  $\text{Mg}_x\text{Ca}_{2-x}(\text{CO}_3)_2$   $0 < x < 1$ ) with modified electronic structure/bond length as detected by  $\mu\text{XAS}$ . At very low Mg concentration bulk calcite was found. Analysis of the data obtained by this comprehensive study provided information on the crystallographic phases, the chemical composition and the crystallinity of the limestone, as summarized in table 1.

From this study we can conclude that the dissolution rate is defined by the concentration of both the fine calcite grains and Mg containing calcite (“modified calcite”). The presence of large crystallites or dolomite phases significantly reduced the reactivity. Therefore for practical applications, the dissolution behavior of material consisting of a pure calcite and Mg containing calcite could be improved by milling. In addition, sieving to the 100-50  $\mu\text{m}$  fraction could help to remove the large dolomite phases for the materials with significant content of fine calcite phases, thereby enhancing their reactivity.

#### 4. Conclusion

The combined study demonstrated that high solubility is provided by small calcite crystals and is furthermore hindered due to the presence of large dolomite crystals. The increase in solubility by removing the dolomite phase via sieving can be therefore successful for some natural limestone materials. These studies provided insight into the microscopic mechanism to tune the reactivity, and in this way might help to optimize this process as well as influence the proper choice of limestone deposits in future.

#### References

- [1] Finck A 2007 *Pflanzenernährung und Düngung* (Baumträger-Verlag, Berlin-Stuttgart)
- [2] Eimer C 2011 *Bewertung von kohlen-sauren Kalkdüngern für die Anwendung in Landwirtschaft, Forst und Gartenbau* Master-Thesis, FH Kiel, FB Agrarwirtschaft
- [3] Grunwaldt H-S „Granulierter Dünge-kalk“, 1980 *Bauernblatt Schleswig-Holstein* 787 - 793.
- [4] Grunwaldt H-S „Neubewertung der Kohlen-sauren Dünge-kalke“ 1986, *Bauernblatt Schleswig-Holstein* 3499 - 3500
- [5] Morse J W and Mackenzie F T 1990 *Geochemistry of Sedimentary Carbonates* (Amsterdam: Elsevier)
- [6] Grunwaldt H-S “Assessment of the Effectiveness of Carbonate Liming Materials, USDA Strategy Meeting, 12.11.2013 Ames/USA, <http://reactivelime.org/4.html> (12.8.2015).
- [7] Hoiberg A “Background and Inconsistencies on Liming Material Evaluation”, USDA Strategy Meeting, 12.11.2013 Ames/USA, <http://reactivelime.org/4.html> (12.8.2015).
- [8] Hugenroth P, Meyer B and Steffens G 1979 *Landw. Forsch.* **32** 157-164
- [9] Hugenroth P and Meyer B 1974 *Landw. Forsch.* **30/I** 160
- [10] Sauerbeck D and Rietz E, 1985 *VDLUFA-Schriften* **16** 431 -438
- [11] Chalmin E, Sansot E, Oriol G, Bousta F and Reiche I 2008 *X-ray Spectrom.* **37** 424
- [12] Brinza L, Schofield P F, Hodson M E, Weller S, Ignatiev K, Geraki K, Quinn P D, Mosselmann J F W 2014 *J. Synchrotron Rad.* **21** 235
- [13] Ilavsky J 2012 *J. Appl. Cryst.* **45** 324.
- [14] Ravel B and Newville M 2005 *J. Synchrotron Rad.* **12** 537–541